Anal. Chem. **2010,** *82,* 6015–6024

Sensitive and Visual Detection of Sequence-Specific DNA-Binding Protein via a Gold Nanoparticle-Based Colorimetric Biosensor

Li-Juan Ou, Pei-Yan Jin, Xia Chu,* Jian-Hui Jiang, and Ru-Qin Yu

State Key Laboratory of Chemo/Bio-Sensing and Chemometrics, College of Chemistry and Chemical Engineering, Hunan University, Changsha 410082, People's Republic of China

A novel exonuclease III (Exo III) protection-based colorimetric biosensing strategy was developed for rapid, sensitive, and visual detection of sequence-specific DNA-binding proteins. This strategy relied on the protection of DNA-cross-linked gold nanoparticle (AuNP) aggregates from Exo III-mediated digestion by specific interactions of target proteins with their binding sequences. Interestingly, we disclosed a new finding that binding of target proteins to their binding sequences in the aggregated AuNP network rendered a stable and long-period protection of DNA. Unlike conventional fluorescence assays merely based on temporal protection of DNA from Exo III digestion, the stable protection afforded a static color transition indicator for DNA−protein interactions with no time-dependent monitoring required in the assay. Therefore, it furnished the developed strategy with improved technical robustness and operational convenience. Furthermore, we introduced thioctic acid as a stable anchor for tethering DNA on AuNPs. This DNA-tethering protocol circumvented the interferences from thiol compounds in common enzymatic systems. The Exo III protection-based colorimetric biosensor was demonstrated using a model target of TATA binding protein, a key transcriptional factor involving in various transcriptional regulatory networks. The results revealed that the method allowed a specific, simple, and quantitative assay of the target protein with a linear response range from 0 to 120 nM and a detection limit of 10 nM.

The detection of sequence-specific DNA-binding proteins is crucial to elucidate gene expression mechanisms and cellular function because of their important roles in transcriptional regulatory networks including transcription, replication, recombination, and repair.[1−3] Moreover, these proteins have long been recognized as attractive markers or targets for disease diagnosis and drug development.[4] As a result, the development of rapid, simple, and robust strategies for detecting sequence-specific DNA-binding proteins and probing their DNA-binding activities is of paramount importance for proteomics, genomics, and biomedicine.

Conventional methods for the detection of sequence-specific DNA-binding proteins include electrophoretic mobility shift assay[5] and DNase footprinting assay.[6] These assays, however, are not only laborious and time-consuming but also require radioisotope or fluorescence labels. Moreover, to render the proteins not dissociated from their binding sequences or ensure most of the DNA molecules are only cut once, experimental conditions in electrophoresis and DNase digestion must be stringently controlled, which makes these techniques challenging in common analytical laboratories. Recent years have witnessed remarkable progress in the design of assay strategies toward rapid detection of DNA-binding proteins. Examples are DNA microarray technology,[7,8] the electrical approach based on DNA-modified electrodes,[9,10] and surface-enhanced Raman scattering.[11] Despite the importance of these techniques, the need for the surface-based immobilization of double-stranded DNA sequences and/or complicated labeling of target proteins can be a detriment. In the context, homogeneous assay approaches, which require neither surface-based operations nor labeling of proteins, then offer a preferable and robust platform for the detection of sequence-specific DNA-binding proteins.

Most existing homogeneous assays of sequence-specific DNA-binding proteins are established on fluorescence techniques.[12−15] A typical strategy is to utilize two double-stranded DNA probes with complementary protruding ends. Two dyes with fluorescence resonant energy transfer (FRET) were labeled separately to these two probes. The interaction between these two double-stranded

* To whom correspondence should be addressed. E-mail: xiachu@hnu.edu.cn. Phone: +86-731-88821916. Fax: +86-731-88821916.

(1) Ren, B.; Robert, F.; Wyrick, J. J.; Aparicio, O.; Jennings, E. G.; Zeitlinger, I. J.; Schreiber, J.; Hannett, N.; Kanin, E.; Volkert, T. L.; Wilson, C. J.; Bell, S. P. *Science* **2000**, *290*, 2306–2309.
(2) Helin, K. *Curr. Opin. Genet. Dev.* **1998**, *8*, 28–35.
(3) Aboussekhra, A.; Biggerstaff, M.; Shivji, M. K.; Vilpo, J. A.; Moncollin, V.; Podust, V. N.; Protic, M.; Hubscher, U.; Egly, J. M.; Wood, R. D. *Cell* **1995**, *80*, 859–868.
(4) Pandolfi, P. P. *Oncogene* **2001**, *20*, 3116–3127.
(5) Garner, M. M.; Revzin, A. *Nucleic Acids Res.* **1981**, *9*, 3047–3060.
(6) Galas, D. J.; Schmitz, A. *Nucleic Acids Res.* **1978**, *5*, 3157–3170.
(7) Bulyk, M. L. *Curr. Opin. Biotechnol.* **2006**, *17*, 422–430.
(8) Berger, M. F.; Philippakis, A. A.; Qureshi, A. M.; He, F. S.; Estep, P. W., III; Bulyk, M. L. *Nat. Biotechnol.* **2006**, *24*, 1429–1435.
(9) Boon, E. M.; Salas, J. E.; Barton, J. K. *Nat. Biotechnol.* **2002**, *20*, 282–286.
(10) Gorodetsky, A. A.; Ebrahim, A.; Barton, J. K. *J. Am. Chem. Soc.* **2008**, *130*, 2924–2925.
(11) Bonham, A. J.; Braun, G.; Pavel, I.; Moskovits, M.; Reich, N. O. *J. Am. Chem. Soc.* **2007**, *129*, 14572–14573.
(12) Furey, W. S.; Joyce, C. M.; Osborne, M. A.; Klenerman, D.; Peliska, J. A.; Balasubramanian, S. *Biochemistry* **1998**, *37*, 2979–2990.
(13) Heyduk, T.; Heyduk, E. *Nat. Biotechnol.* **2002**, *20*, 171–176.
(14) Xu, X.; Zhao, Z.; Qin, L.; Wei, W.; Levine, J. E.; Mirkin, C. A. *Anal. Chem.* **2008**, *80*, 5616–5621.
(15) Wang, J.; Li, T.; Guo, X.; Lu, Z. *Nucleic Acids Res.* **2005**, *33*, 2–9.

10.1021/ac100907g
Published on Web 06/21/2010

DNA probes and the binding protein will promote the annealing of the complementary protruding ends with a FRET signal generated.[13] This technique is conceptually simple and rapid. It, however, seems to suffer the limitation that the split of a protein-binding sequence may substantially affect the binding affinity, especially for the proteins with small binding sites. An alternative approach is to exploit a DNA duplex with a FRET pair on each strand.[14,15] Specific binding of target proteins to the binding sequence will protect the DNA duplex from digestion by exonuclease III (Exo III) with the FRET signal retained.[14,15] Such an Exo III protection-based fluorescence assay offers a simple and flexible approach for probing the DNA−protein interactions without complicated labeling of target proteins and deliberate splitting of protein-binding sequences. Nevertheless, because Exo III usually nibbles into the protein-bound DNA segment and even displaces some DNA-binding proteins, it is highly demanding to resort to real-time monitoring of the digestion reaction for achieving a robust Exo III protection-based assay.[14−16] Therefore, the development of more reliable and convenient strategies for DNA-binding protein assays still remains a grand challenge.

Gold nanoparticle (AuNP)-based colorimetric assays have attracted fast-growing interest in recent years because of their high sensitivity comparable to fluorescence assay and exquisite capability of visual detection using "naked" eyes.[17,18] AuNPs display a unique distance-dependent optical property, which has been widely adopted as a colorimetric bioanalytical platform for varying applications. Typical implementations include biosensors for different targets such as DNA,[19−21] metal ions,[22,23] small molecules,[24−28] proteins,[29−32] and even cancer cells,[33] as well as drug screening for DNA binders[34−36] and enzyme assays.[37−39] With the integration of varying enzymatic reactions of DNA and RNA such as cleavage, ligation, and polymerization, this platform has been able to greatly expand our capacity to smart design new bioanalytical platforms.[36−44] For instance, by using exonuclease I-based manipulation, a colorimetric biosensor was able to be implemented for evaluating the stabilization of G-quadruplex selectively mediated by small ligands.[36] In addition, biosensors specific for Pb^{2+} and UO_2^{2+} were developed based on the metal ion-dependent DNAzymes.[40,41] Colorimetric biosensor platforms were also proposed for monitoring enzymatic activity and screening of inhibitors of endonuclease.[37,42] The platform, based on nickase-assisted amplification, was demonstrated to be useful for ultrasensitive and selective detection of DNA.[43] We previously demonstrated a DNA ligase based strategy for colorimetric detection of single-nucleotide mutation.[44] Despite the successes, the implementation of AuNP-based colorimetric biosensors for enzymatic systems is frequently confronted with a technical difficulty that thiolated oligonucleotides tethered on AuNPs will be displaced by thiol compounds, reagents commonly present in storage and/or reaction solutions in such systems. Recently, others and we demonstrated that thioctic acid, a common cyclic disulfide agent, could serve as stable anchors for DNA strands on AuNPs in preventing the displacement by thiol compounds.[45,46] This expands the possibilities of DNA-modified AuNPs as a competent biosensing platform for enzymatic systems.

Herein we developed a novel, rapid, robust, and convenient colorimetric biosensing strategy for detecting sequence-specific DNA-binding proteins based on Exo III protection-based assays. This strategy relied on the protection of DNA-cross-linked AuNP aggregates from Exo III-mediated digestion by specific interactions of target proteins with their binding sequences. To the best of our knowledge, this strategy was the first example of a colorimetric biosensor for visual detection of sequence-specific DNA-binding proteins. Interestingly, we disclosed a new finding that binding of target proteins to their binding sequences in the aggregated AuNP network rendered a stable and long-period protection of the double-stranded DNA, which was contrasted substantially with the temporal protection of double-stranded DNA in fluorescence assays.[14,15] This finding actually implied our assay could achieve a static color transition indicator for DNA−protein binding and require no time-dependent monitoring of the reaction. Consequently, the developed strategy was able to afford improved technical robustness and operational convenience as compared to the fluorescence-based Exo III protection assay. In addition,

(16) Metzger, W.; Heumann, H. In *Footprinting with Exonuclease III*; Moss, T., Ed.; Humana Press Inc.: Totowa, NJ, 2001; pp 39−47.
(17) Storhoff, J. J.; Lazarides, A. A.; Mucic, R. C.; Mirkin, C. A.; Letsinger, R. L.; Schatz, G. C. *J. Am. Chem. Soc.* **2000**, *122*, 4640–4650.
(18) Zhao, W.; Brook, M. A.; Li, Y. *ChemBioChem* **2008**, *9*, 2363–2371.
(19) Xu, W.; Xue, X.; Li, T.; Zeng, H.; Liu, X. *Angew. Chem., Int. Ed.* **2009**, *48*, 6849–6852.
(20) Elghanian, R.; Storhoff, J. J.; Mucic, R. C.; Letsinger, R. L.; Mirkin, C. A. *Science* **1997**, *277*, 1078–1080.
(21) Hazarika, P.; Ceyhan, B.; Niemeyer, C. M. *Angew. Chem., Int. Ed.* **2004**, *43*, 6469–6471.
(22) Xue, X.; Wang, F.; Liu, X. *J. Am. Chem. Soc.* **2008**, *130*, 3244–3245.
(23) Lee, J.-S.; Han, M. S.; Mirkin, C. A. *Angew. Chem., Int. Ed.* **2007**, *46*, 4093–4096.
(24) Liu, J.; Lu, Y. *Angew. Chem., Int. Ed.* **2006**, *45*, 90–94.
(25) Zhao, W.; Chiuman, W.; Brook, M. A.; Li, Y. *ChemBioChem* **2007**, *8*, 727–731.
(26) Zhao, W.; Chiuman, W.; Lam, J. C. F.; McManus, S. A.; Chen, W.; Cui, Y.; Pelton, R.; Brook, M. A.; Li, Y. *J. Am. Chem. Soc.* **2008**, *130*, 3610–3618.
(27) Liu, J.; Lu, Y. *J. Am. Chem. Soc.* **2007**, *129*, 8634–8643.
(28) Han, M. S.; Lytton-Jean, A. K. R.; Oh, B.-K.; Heo, J.; Mirkin, C. A. *Angew. Chem., Int. Ed.* **2006**, *45*, 1807–1810.
(29) Huang, C.-C.; Huang, Y.-F.; Cao, Z.; Tan, W.; Chang, H.-T. *Anal. Chem.* **2005**, *77*, 5735–5741.
(30) Pavlov, V.; Xiao, Y.; Shlyahovsky, B.; Willner, I. *J. Am. Chem. Soc.* **2004**, *126*, 11768–11769.
(31) Hong, S.; Choi, I.; Lee, S.; Yang, Y. I.; Kang, T.; Yi, J. *Anal. Chem.* **2009**, *81*, 1378–1382.
(32) Xu, H.; Mao, X.; Zeng, Q.; Wang, S.; Kawde, A.-N.; Liu, G. *Anal. Chem.* **2009**, *81*, 669–675.
(33) Liu, G.; Mao, X.; Phillips, J. A.; Xu, H.; Tan, W.; Zeng, L. *Anal. Chem.* **2009**, *81*, 10013–10018.
(34) Han, M. S.; Lytton-Jean, A. K. R.; Oh, B.-K.; Heo, J.; Mirkin, C. A. *Angew. Chem., Int. Ed.* **2006**, *45*, 1807–1810.
(35) Hurst, S. J.; Han, M. S.; Lytton-Jean, A. K. R.; Mirkin, C. A. *Anal. Chem.* **2007**, *79*, 7201–7205.
(36) Chen, C.; Zhao, C.; Yang, X.; Ren, J.; Qu, X. *Adv. Mater.* **2009**, *21*, 1–5.
(37) Xu, X.; Han, M. S.; Mirkin, C. A. *Angew. Chem., Int. Ed.* **2007**, *46*, 3468–3470.
(38) Liu, T.; Zhao, J.; Zhang, D.; Li, G. *Anal. Chem.* **2010**, *82*, 229–233.
(39) Zhao, W.; Ali, M. M.; Aguirre, S. D.; Brook, M. A.; Li, Y. *Anal. Chem.* **2008**, *80*, 8431–8437.
(40) Liu, J.; Lu, Y. *J. Am. Chem. Soc.* **2004**, *126*, 12298–12305.
(41) Lee, J. H.; Wang, Z.; Liu, J.; Lu, Y. *J. Am. Chem. Soc.* **2008**, *130*, 14217–14226.
(42) Zhao, W.; Lam, J. C. F.; Chiuman, W.; Brook, M. A.; Li, Y. *Small* **2008**, *4*, 810–816.
(43) Xu, W.; Xue, X.; Li, T.; Zeng, H.; Liu, X. *Angew. Chem., Int. Ed.* **2009**, *48*, 6849–6852.
(44) Li, J.; Chu, X.; Liu, Y.; Jiang, J. H.; He, Z.; Zhang, Z.; Shen, G.; Yu, R. Q. *Nucleic Acids Res.* **2005**, *33*, e168.
(45) Letsinger, R. L.; Elghanian, R.; Viswanadham, G.; Mirkin, C. A. *Bioconjugate Chem.* **2000**, *11*, 289–291.
(46) Huang, Y.; Zhang, Y. L.; Xu, X.; Jiang, J. H.; Shen, G. L.; Yu, R. Q. *J. Am. Chem. Soc.* **2009**, *131*, 2478–2480.

Table 1. Synthesized Oligonucleotides (5′ → 3′) Used in the Experiments[a]

sense strand **1**	NH_2-T_{20} CAC G**TA TAA AG**G ATC ACA CTA GCA C*TT TTT*
antisense strand **2**	NH_2-T_{10} GTG CTA GTG TGA TC**C TTT ATA** CGT G
mutant sense strand **3**	NH_2-T_{20} CAC G**GA TAA AG**G ATC ACA CTA GCA C*TT TTT*
mutant antisense strand **4**	NH_2-T_{10} GTG CTA GTG TGA TC**C TTT ATC** CGT G
mutant sense strand **5**	NH_2-T_{20} CAC G**TA CAA AG**G ATC ACA CTA GCA C*TT TTT*
mutant antisense strand **6**	NH_2-T_{10} GTG CTA GTG TGA TC**C TTT GTA** CGT G
hairpin DNA **7**	GGT G**CT TTA TA**T TGG GTA GGG CGG GTT TTT TCC CGC CCT ACC CAA **TATA AAG** CAC C
sense strand **8**	NH_2-T_{20} CAC G**TA TAA AG**G ATC ACA CTA GCA C*TT TTT*–FITC

[a] The boldface portions indicate the TATA binding protein-binding site. The underlined letters symbolize mutant bases in the TATA binding protein-binding site. Five protruding bases (italicized T) at the 3′-end of each sense strand were used to prevent the sense strands from the digestion of the Exo III.

we introduced thioctic acid as a stable anchor for tethering DNA on AuNPs. This DNA-tethering protocol circumvented the interference from thiol compounds in storage and reaction buffers for Exo III. In the present study, the Exo III protection-based colorimetric assay was demonstrated using a model target of TATA binding protein, a key transcriptional factor involved in many important transcriptional regulatory networks.[47] The results revealed that the developed method held great potential as a sensitive, robust, and convenient platform for the detection of sequence-specific DNA-binding proteins.

EXPERIMENTAL SECTION

Reagents and Materials. TATA binding protein was purchased from Protein One, Inc. (Bethesda, MD). *E. coli* Exo III and methyltransferase *Hha*I (M.*Hha*I) were obtained from New England Biolabs (Ipswich, MA). *N*-Hydroxysulfosuccinimide (sulfo-NHS), 1-ethyl-3-(3-dimethylaminopropyl) carbodiimide hydrochloride (EDC), thioctic acid, and full-length human p53 protein were from Sigma-Aldrich Chemical Co. SYBR Green I (supplied as 10 000×) was obtained from Molecular Probes. Bovine serum albumin (BSA) was provided by Dingguo Biotechnology Co. Ltd. (Beijing, China). Trisodium citrate, KH_2PO_4, Na_2HPO_4, and NaCl were from Amresco (Solon, OH). Other reagents were all purchased from Sinopharm Chemical Reagent Co., Ltd. (Shanghai, China). All solutions were prepared using ultrapure water, which was obtained through a Millipore Milli-Q water purification system (Billerica, MA) and had an electrical resistance of >18.3 MΩ. The oligonucleotides used in this work were synthesized from Takara Biotechnology Co. Ltd. (Dalian, China). The thermodynamic parameters of all oligonucleotides were calculated using bioinformatics software[48] (http://www.bioin-fo.rpi.edu/applications/). The sequences of the synthesized oligonucleotides are given in Table 1.

Preparation of Citrate-Capped AuNPs. Citrate-capped AuNPs were prepared by citrate reduction of $HAuCl_4$ according to documented protocols,[49,50] as briefly described as follows: Trisodium citrate (10 mL, 38.8 mM) was added rapidly to a stirred boiling solution of $HAuCl_4$ (100 mL, 1 mM). Within several minutes, the color of the solution changed from pale yellow to deep red. The solution was heated under reflux for another 30 min to ensure complete reduction, and it was then slowly cooled to room temperature and stored at 4 °C before use. The average size of the Au nanoparticles was 13 ± 2 nm as calculated from the transmission electron microscopy (TEM) image. The concentration of these AuNPs was determined to be ~13 nM based on an extinction coefficient of 2.7×10^8 M^{-1} cm^{-1} at 520 nm for 13 nm AuNPs[50] using UV−vis absorption spectroscopy (UV 2450, Shimadzu, Kyoto, Japan). Because of the citrate reduction method could yield Au nanoparticles with desirably uniform size, it was found that very good reproducibility was obtained in the assay even using Au nanoparticles prepared in different runs.

Conjugation of Amino-Labeled Oligonucleotides to Thioctic Acid. The conjugation of thioctic acid to NH_2-modified oligonucleotides was performed using the succinimide coupling (EDC−NHS) method.[46,51] Briefly, 100 μL of 10 μM NH_2-modified oligonucleotide (see Table 1 for their sequences) was mixed with 100 μL of 10 mM phosphate-buffered saline (PBS, 10 mM phosphate buffer, 0.3 M NaCl, pH 7.4) containing 10 mM of thioctic acid, 1 mM EDC, and 5 mM sulfo-NHS and incubated for 2 h at 37 °C. The conjugate was dialyzed against 10 mM PBS (500 mL) for 3 days in the dark to remove excessive thioctic acid.

Preparation of DNA-Modified AuNPs. AuNPs were modified with DNA oligonucleotides conjugated to thioctic acid according to documented methods with slight modifications.[49,50] Briefly, the thioctic acid-conjugated oligonucleotides (200 μL, 5 μM) were added in the citrate-capped AuNP solution (1 mL, ~13 nM). After 18 h, the solution was mixed with 1.2 mL of phosphate buffer (PB, pH 7.4, 10 mM) containing 0.1 M NaCl for 8 h. In the subsequent salt aging process, AuNP solution was first incubated in 0.1 M NaCl for 8 h, then salted to 0.2 M NaCl for further incubating for 8 h, and finally salted to 0.3 M NaCl for 8 h. The unmodified oligonucleotides were removed via centrifugation at 22 000*g* for 20 min followed by resuspension of the sediment in 1 mL of PBS (10 mM PB, 0.3 M NaCl, pH 7.4). This step was repeated three times to sufficiently remove all excess oligonucleotides. Then, the DNA-modified AuNPs were redispersed in 1 mL of PBS (10 mM PB, 0.3 M NaCl, pH 7.4) and stored at 4 °C until use. The final concentration of DNA-modified AuNPs is ~13 nM, assuming that the loss of AuNPs was negligible during the preparation process.

To quantify the DNA concentration on each AuNP after modification, a thioctic acid-conjugated oligonucleotide with a fluorescein isothiocyanate (FITC) tag (sequence 8 in Table 1) was used to modify AuNPs according to the aforementioned protocol. It could be assumed that the surface coverage of the FITC-tagged oligonucleotide was the same as those for other DNA-modified AuNPs because of the same modification chemistry. To determine the amount of FITC-tagged oligonucleotide in the as-prepared AuNP solution, in 100 μL of DNA-modified AuNP solution, 20 μL

(47) Hernandez, N. *Genes Dev.* **1993**, *7*, 1291–1308.
(48) Zuker, M. *Nucleic Acids Res.* **2003**, *31*, 3406–3415.
(49) Liu, J.; Lu, Y. *Nat. Protoc.* **2006**, *1*, 246–252.
(50) Hill, H. D.; Mirkin, C. A. *Nat. Protoc.* **2006**, *1*, 324–336.
(51) Zhang, Y. L.; Huang, Y.; Jiang, J. H.; Shen, G. L.; Yu, R. Q. *J. Am. Chem. Soc.* **2007**, *129*, 15448–15449.

of 0.2 M KCN, and 2 mM $K_3Fe(CN)_6$ was added to dissolve AuNPs and release the FITC-tagged oligonucleotides. Then, the released FITC-modified oligonucleotide was quantified using three standard solutions of the FITC-modified oligonucleotide. On the basis of triplicate assays of the as-prepared AuNP solution, the surface concentration of oligonucleotide was estimated to be 183 ± 20 strands per AuNP. This gave an effective final DNA concentration of 0.9 ± 0.1 μM in the AuNP solution.

Preparation of DNA-Cross-Linked AuNP Aggregates. Typically, the sense strand and the complementary antisense strand-modified AuNPs (50 μL each, ~13 nM) in PBS (10 mM PB, 0.3 M NaCl, pH 7.4) were mixed. The mixture was heated to 70 °C and incubated for 10 min, followed by slow cooling to room temperature (over ~2 h). Such treatments resulted in the hybridization of these two AuNP-labeled oligonucleotides with a concomitant red-to-purple color change. Then, the DNA-cross-linked AuNP aggregates thus obtained were washed three times with a reaction buffer containing 10 mM Tris−HCl (pH 7.0), 4 mM $MgCl_2$, and 10 μM dithiothreitol (DTT) by centrifugation at 8000*g* for 5 min. The precipitate was resuspended in 100 μL of the reaction buffer containing 10 mM Tris−HCl (pH 7.0), 4 mM $MgCl_2$, and 10 μM DTT.

Exo III Protection-Based Colorimetric Assay of TATA Binding Protein. A 2 μL aliquot of sample solution containing varying concentrations of TATA binding protein was added in a solution (50 μL) of the as-prepared DNA-cross-linked AuNP aggregates and incubated at 37 °C for 30 min to allow equilibrium binding. Then, 8 U μL^{-1} of Exo III was added, and the digestion reaction in the system was monitored by UV−vis absorption spectroscopy (Shimadzu UV-2450, Kyoto, Japan) or directly visualized using naked eyes. The absorption spectroscopic measurements were performed at room temperature in a 50 μL quartz cuvette. To ensure homogeneity of the particle suspension, all solutions were agitated vigorously before absorption spectra were recorded.

Characterization Experiments. The hydrodynamic sizes of DNA-modified AuNPs and the DNA-cross-linked AuNP aggregates were determined by dynamic light scattering using a Malvern Zetasizer 3000 HS particle size analyzer (Malvern Instruments, Worcs, U.K.). Transmission electron microscopy was also used to characterize the sizes of the DNA-modified AuNPs and the DNA-cross-linked AuNP aggregates. Samples were prepared by dropping the sample solution (4 μL) onto a carbon-coated copper grid. The solution was wicked from the edge of the grid with a piece of filter paper after 1 min. Transmission electron microscopy images were taken with a Hitachi TEM 800 (Japan).

The capillary electrophoresis (CE) experiment was performed using a capillary electrophoresis system equipped with UV absorption detection (P/AGE MDQ, Beckman, Germany) under an applied potential of 15 kV using a quartz capillary with 75 μm diameter (total length, 50 cm; effective length, 30 cm) in 50 mM borate running buffer (pH 9.2). The DNA-cross-linked AuNP aggregates were digested by Exo III (40 U μL^{-1}) in the presence or absence of TATA binding protein (2.5 μM). The resulting solution was centrifuged at 22 000*g* for 20 min followed by injecting the supernatant into the capillary using the pressure injection mode at 0.5 psi for 5 s and detected at 254 nm for 30 min. The temperature of the separation, 25 °C, was controlled by immersion of the capillary in a cooling liquid circulating in the cartridge. Between successive runs, the capillary was rinsed with ultrapure water and running buffer for 15 min, respectively.

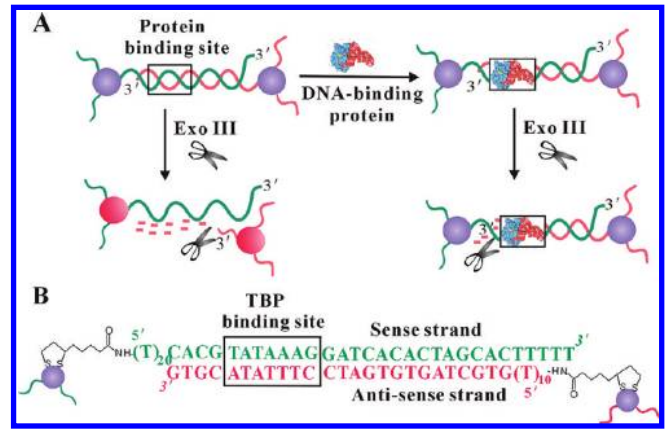

Figure 1. (A) Schematic illustration of Exo III protection-based colorimetric biosensor for detecting DNA-binding protein. (B) Sequences of the sense and the antisense strands for the detection of TATA binding protein. The black square indicates the TATA binding protein-binding sites. Five protruding nucleotides (dT) were incorporated at the 3′-end of the sense strand to protect the sense strand from Exo III digestion and ensure a unidirectional degradation along the recessed end of the antisense strand.

Exo III protection-based fluorescence assay of TATA binding protein with SYBR Green I as the duplex staining agent was performed at room temperature in a 384-well black microplate (30 μL) on a Tecan Infinite M 1000 microplate reader (Switzerland). The excitation and emission wavelengths were set to 497 and 525 nm, respectively.

RESULTS AND DISCUSSION

Design of Exo III Protection-Based Colorimetric Biosensing Strategy. Figure 1 illustrates the general principle of the Exo III protection-based colorimetric biosensing strategy for the detection of sequence-specific DNA-binding protein. Two oligonucleotides, the sense and the antisense strands, are designed with complementary sequences. These two oligonucleotides are tethered on AuNP surface via the thioctic acid anchor such that they are stable in enzymatic reaction solutions containing DTT. Hybridization of these two oligonucleotides results in the formation of AuNP aggregates that are cross-linked by the DNA duplex between the complementary sequences. A red-to-purple color change of the solution is obtained as an indicator for the formation of the AuNP aggregates. The DNA duplexes formed among the AuNP aggregates contain the consensus sequence of the target DNA-binding protein. In the absence of the DNA-binding protein, Exo III, a double-strand-specific 3′ to 5′ exodeoxyribonuclease, will stepwisely and nonprocessively digest the double-stranded DNA from the 3′ recessed ends of the antisense strands.[52] This causes the dissociation of the AuNP aggregates into dispersed AuNPs with a concomitant purple-to-red color change for the solution. In the presence of the DNA-binding protein, tight binding of the proteins to the consensus sequences induces steric hindrance to Exo III in approaching the 3′-termini, which protects the antisense strands from Exo III-mediated digestion. This retains

(52) Thomas, K. R.; Olivery, B. M. *J. Biol. Chem.* **1978**, *253*, 424–429.

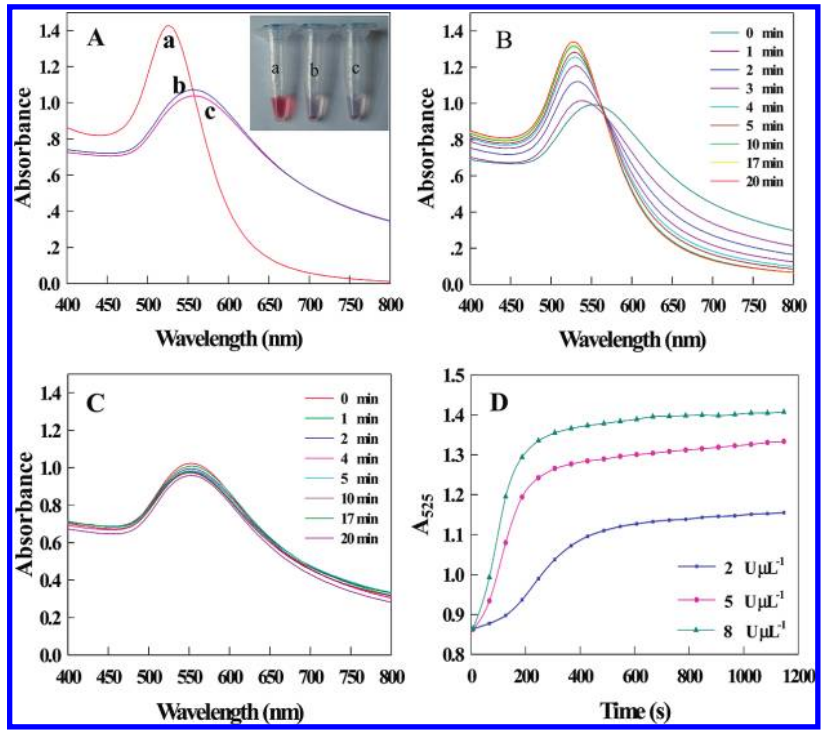

Figure 2. (A) Absorption spectra obtained for AuNP aggregate solution after digestion by Exo III (a), for AuNP aggregate solution (b), and for AuNP aggregate solution after digestion by inactivated Exo III (c). The inset is the photograph for the corresponding systems. (B) Absorption spectra obtained in monitoring the digestion of AuNP aggregates by Exo III. (C) Absorption spectra obtained in monitoring the digestion of AuNP aggregates by inactivated Exo III. (D) Time-dependent absorbance responses obtained in monitoring the digestion of AuNP aggregates by 2, 5, and 8 U μL^{-1} Exo III.

stable AuNP aggregates in the solution with no color change obtained. On the basis of this principle, the presence of DNA-binding proteins is translated into the protection of the DNA-cross-linked AuNP aggregates from Exo III-mediated digestion. Since the degradation of the DNA-cross-linked AuNP aggregates can be detected immediately using "naked" eyes or quantified using absorption spectral measurements, the developed technique then offers a convenient strategy for colorimetric detecting of the DNA-binding proteins.

It should be noted that the following aspects were of key importance in the design of the Exo III protection-based colorimetric biosensor. First, there were long spacers at the 5′-end of both the DNA strands tethered on AuNPs, 20 and 10 dT nucleotides, respectively, for the sense and the antisense strands. Shorter spacers would substantially reduce the degradation of the DNA-cross-linked AuNP aggregates by Exo III because of relatively high steric hindrance in the cross-linked AuNP networks. Second, five protruding nucleotides (dT) was incorporated at the 3′-end of the sense strand. This allows the protection of the sense strands from Exo III-mediated digestion and ensured a unidirectional degradation of the double-stranded DNA. Because bidirectional digestion from the 3′-ends of both the sense and the antisense strands might degrade the double-stranded DNA into short fragments, the AuNP aggregates would also become dissociated even in the presence of DNA-binding proteins. So, such a design of the sense strand with a protruding end provided a simple route to combat the false signals arising from bidirectional digestion by Exo III. Third, a cyclic disulfide anchor of thioctic acid was employed for immobilizing the DNA strands on AuNPs. This improved the stability of the surface-tethered DNA strands and prevented their displacement by thiol compounds in enzymatic systems.

Digestion of DNA-Cross-Linked AuNP Aggregates by Exo III. A central hypothesis of the colorimetric biosensor is that Exo III can effectively degrade double-stranded DNA embedded in the AuNP aggregates. To validate the hypothesis, we first investigated the digestion reaction of the DNA-cross-linked AuNP aggregates by Exo III. The sense strand and the antisense strands were designed toward a model sequence-specific DNA-binding protein, TATA binding protein, a key transcription factor and an essential component for transcription initiation by all nuclear RNA polymerases.[47] The consensus sequence of TATA binding protein is TATAAAG, as shown in Figure 1B. When two AuNPs modified with these two DNA strands were mixed for hybridization, we obtained purple-colored DNA-cross-linked AuNP aggregates with a broad surface plasmon absorption peak at ~550 nm. This observation was in coincidence with previous reports.[17]

Figure 2 depicts the absorption spectral readings obtained in monitoring the digestion of the DNA-cross-linked AuNP aggregates by Exo III. In the absence of Exo III, the purple AuNP aggregates were gradually subsided to the bottom of the microcentrifuge tube, and after 60 min the supernatant became almost colorless. By agitating of the solution, we obtained an absorption spectrum with a broad absorption peak at ~550 nm for the AuNP aggregates. After adding Exo III in the system, the solution exhibited an obvious purple-to-red color change after a 10 min digestion, and a narrow absorption peak at ~525 nm for dispersed AuNPs was observed in place of the broad absorption peak at ~550 nm of the AuNP aggregates (Figure 2A, curves a and b). As a control, Exo III was inactivated by heating at 70 °C for 20

min and then introduced in the system. In this case, one also obtained purple AuNP precipitates after a 60 min incubation with an almost colorless supernatant. The corresponding absorption spectrum did not display significant variations from that for the system without Exo III (Figure 2A, curves b and c). This observation verified that Exo III could work in the DNA-cross-linked AuNP networks and effectively degrade the double-stranded DNA, resulting in the dissociation of the AuNP aggregates. The control experiment with inactivated Exo III suggested that the transition from purple AuNP aggregates into red AuNPs was derived from the digestion reaction mediated by active Exo III rather than coexisting compounds in the storage buffer for Exo III.

Time-dependent monitoring of the Exo III-mediated digestion reaction of the DNA-cross-linked AuNP aggregates was performed using the absorption spectroscopy (Figure 2, parts B and C). It was found that, immediately after the addition of 8 U μL^{-1} Exo III, the surface plasmon band was rapidly blue-shifted from ~550 to ~525 nm with a concomitant substantial increase in the absorbance at 525 nm. After a 10 min reaction, the changes of color and absorption spectra became very slow, and a homogeneous red-colored solution with a stable surface plasmon band was obtained after a 20 min digestion (Figure 2B). In contrast, after the addition of thermally inactivated Exo III, there were no remarkable changes in the absorption spectra in a 20 min reaction, indicating that the AuNP aggregates remained stable in inactivated Exo III solution (Figure 2C).

Kinetic studies were then performed to inspect the effect of varying concentrations of Exo III on the digestion reactions by monitoring the absorbance at 525 nm as a function of time (Figure 2D). It was clear that, with low Exo III concentration (2 U μL^{-1}), the absorbance was elevated at a low rate in the initial stage followed by a stagnant increase after 6 min, indicating that the DNA-cross-linked AuNP aggregates were degraded at low efficiency. Note that such an Exo III concentration (2 U μL^{-1}) was sufficient for effective digestion of double-stranded DNA structures.[14,15] Thus, this observation actually implied that the steric hindrance of the DNA-cross-linked AuNP aggregates had a dramatic effect on the activity of Exo III. With 5 U μL^{-1} Exo III, we observed a much higher digestion rate for the DNA-cross-linked AuNP aggregates. At higher Exo III concentration of 8 U μL^{-1}, the degradation rate was found to be further elevated. These findings revealed that the activity loss of Exo III arising from the steric hindrance could be compensated for by the use of high-concentration Exo III, which allowed efficient degradation of the DNA-cross-linked AuNP aggregates. Since 8 U μL^{-1} Exo III was able to rapidly degrade the AuNP aggregates (within 20 min), this concentration was chosen in the assay.

To obtain maximized differentiation in solution colors and absorption spectra between the dispersed AuNPs and the AuNP aggregates, attempts were made to use shorter spacers, say 10 and 0 dT nucleotides at the 5′-end for the sense and the antisense strands, respectively, in place of 20 and 10 dT nucleotides.[17] Surprisingly, no color change and spectral shift were observed after the digestion of the AuNP aggregates even using Exo III of a concentration as high as 16 U μL^{-1}. Presumably, this seemed attributed to the fact that the steric hindrance in the AuNP networks cross-linked by the DNA strands with shorter spacers was so severe that Exo III could not approach the 3′-termini of the antisense strands.

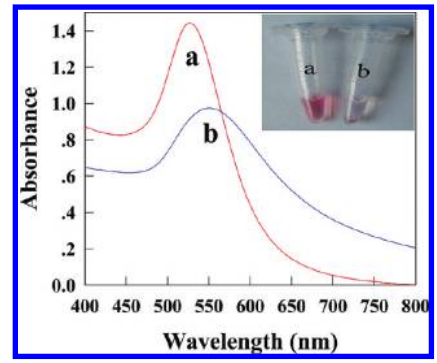

Figure 3. Absorption spectra obtained for AuNP aggregates cross-linked by TATA binding protein cognate sequences after a 20 min digestion by Exo III in the absence (a) and presence (b) of 500 nM TATA binding protein. The inset is the photograph for the corresponding systems.

It is noteworthy that, because of the cross-linking structure of the AuNP aggregates, there is more severe steric hindrance in the interior of the aggregates than in the exterior. Such increased steric hindrance in the interior of the aggregates will prevent Exo III from rapidly penetrating into the network and efficiently degrading the DNA population in the core of the AuNP aggregates. Therefore, it is supposed that the population of DNA strands in Au nanoparticle aggregates is digested fast in the exterior of the AuNP aggregates, while it is degraded relatively slowly in the interior of the aggregates.

Exo III Protection-Based Colorimetric Biosensor for TATA Binding Protein Detection. After investigating the digestion reactions of the AuNP aggregates by Exo III, these aggregates were used to probe the interaction of TATA binding protein with sequence-specific DNA. The AuNP aggregates were incubated with 500 nM TATA binding protein at 37 °C for 30 min followed by the digestion by Exo III at room temperature for 20 min. As expected, in the presence of 500 nM TATA binding protein, no color change and absorption spectral shift were observed after the Exo III-mediated digestion (Figure 3b). In contrast, an obvious purple-to-red color change and appreciable absorption spectral shift occurred in the absence of TATA binding protein (Figure 3a). This implied that the sequence-specific DNA-binding protein, e.g., TATA binding protein, protected the AuNP aggregates from Exo III-mediated digestion, which was presumably attributed to the steric hindrance from the tightly bound DNA−protein complexes.

To further validate this finding, the specificity of DNA−protein interaction was investigated by using noncognate sequences of the TATA protein-binding site and noncognate proteins of the sequence. First, to explore the effect of the noncognate sequences of the TATA protein-binding site, we changed T1 and T3 positions in the consensus TATA protein-binding site to G1 and C3, respectively, and prepared the corresponding AuNP aggregates (Figure 4B). These AuNP aggregates were incubated with TATA binding protein at 37 °C for 30 min and then digested by Exo III at room temperature for 20 min. As clearly shown in Figure 4A, the AuNP aggregates cross-linked by the noncognate sequences of the TATA binding protein-binding site displayed an obvious

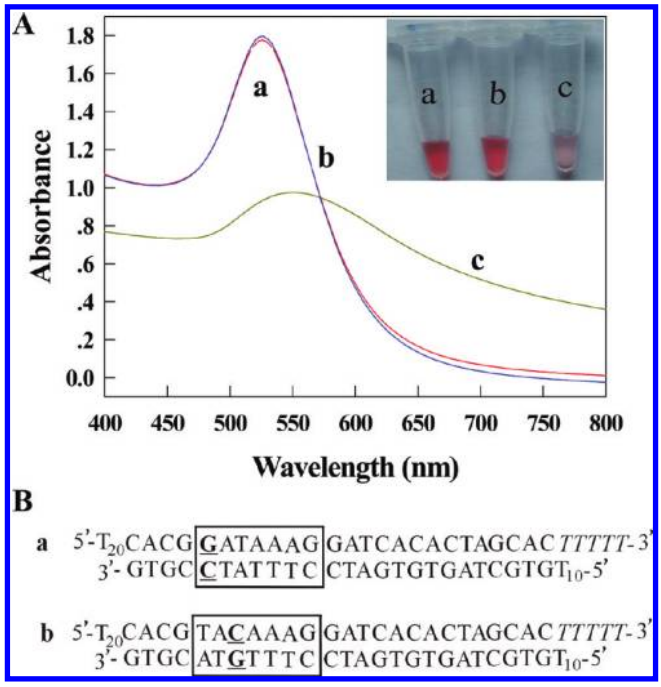

Figure 4. (A) Absorption spectra obtained after a 20 min digestion by Exo III in the presence of 500 nM TATA binding protein for AuNP aggregates cross-linked by TATA binding protein noncognate sequence with T1 mutated to G1 (a), TATA binding protein noncognate sequence with T3 mutated to C3 (b), and TATA binding protein cognate sequences (c). The inset is the photograph for the corresponding systems. (B) Sequences of noncognate sequence 1 (a) and 2 (b). Underlined letters represent the base different from the cognate sequence embraced in the squares.

color change and absorption spectral shift after the Exo III-mediated digestion even in the presence of 500 nM TATA binding protein (curves a and b). In contrast, the interaction of the AuNP aggregates containing the cognate sequence of TATA binding protein with TATA binding protein prevented the degradation with no color change and spectral shift obtained. This confirmed that the protection of the AuNP aggregates from Exo III-mediated digestion is arising from specific binding of TATA binding protein to its recognition sequence rather than nonspecific adsorption of the protein to the noncognate DNA sequences.

Second, the specificity of the colorimetric biosensor for the detection of TATA binding protein was demonstrated by using noncognate proteins. BSA, a protein that did not strongly interact with DNA, M.*Hha*I that recognized and catalyzed the methylation of cytosine in a four-nucleotide DNA sequence 5′-GCGC-3′, and p53 protein that specifically bound to a 10-nucleotide DNA sequences, were selected as the noncognate proteins to perform the experiments. The AuNP aggregates containing the TATA binding protein recognition site were incubated with BSA, M.*Hha*I, and p53 protein, respectively, in the absence and presence of TATA binding protein, and then digested by Exo III. As shown in Figure 5, an obvious color change and remarkable spectral shift were observed when the AuNP aggregates were incubated only with one of the noncognate proteins in the absence of TATA binding protein. In the presence of TATA binding protein and one of the noncognate proteins, protection of the AuNP aggregates was obtained with no color change, and spectral shift occurred. This further confirmed that proteins not binding to the recognition sequence would not protect the AuNP aggregates from Exo III-mediated digestion, and these proteins would also not interfere with the specific binding of TATA binding protein to its recognition site.

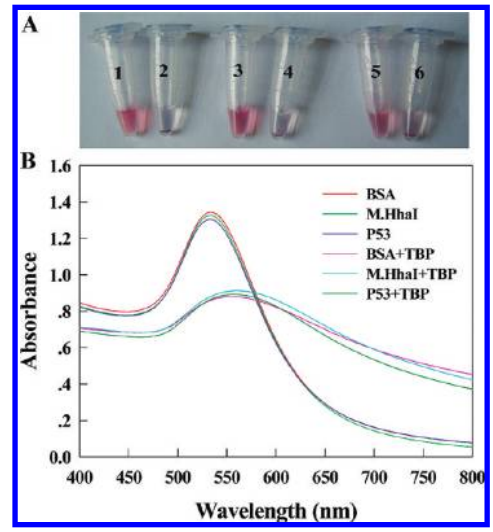

Figure 5. (A) Photograph obtained after Exo III-mediated digestion of AuNP aggregates in the presence of 2 μM BSA (1), 2 μM BSA plus 500 nM TATA binding protein (2), 500 nM M.*Hha*I (3), 500 nM M.*Hha*I plus 500 nM TATA binding protein (4), 500 nM p53 (5), and 500 nM p53 plus 500 nM TATA binding protein (6). (B) Absorption spectra of the corresponding systems.

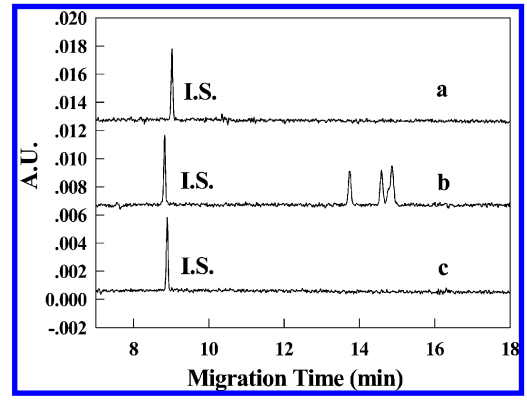

Figure 6. Electropherograms of supernatants obtained by centrifuging AuNP aggregates (a), AuNP aggregates digested by 40 U μL^{-1} Exo III (b), and AuNP aggregates incubated with 2.5 μM TATA binding protein followed by digestion of 40 U μL^{-1} Exo III (c). The internal standard is 80 μM adenosine.

Characterization of the Exo III Protection-Based Colorimetric Biosensor. To further verify our findings that the DNA-cross-linked AuNP aggregates could be degraded by Exo III and the interaction of DNA-binding protein with its recognition site could protect the AuNP aggregates from Exo III-mediated digestion, CE experiments were performed. The AuNP aggregates were concentrated by 5-fold and incubated in the presence or absence of 2.5 μM TATA binding protein followed by Exo III-mediated digestion. The resultant mixtures were centrifuged under 22 000*g* for 20 min, and the supernatants obtained were injected into the CE system for analysis (Figure 6). Because of the limited working concentrations and absorption coefficients of the proteins at 254 nm, the peaks appearing in the electropherograms were exclusively arising from the DNA hydrolysis products. The supernatant of the AuNP aggregates did not give any peaks other than the internal standard. In contrast, three peaks appeared behind the

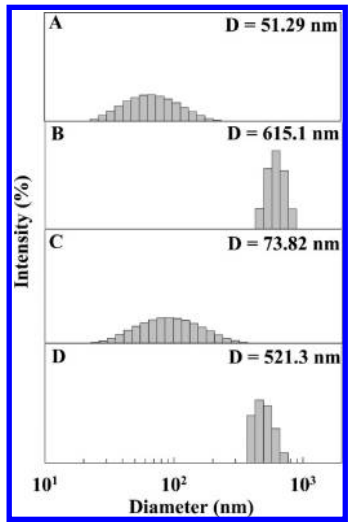

Figure 7. Size distributions of DNA-modified AuNPs (A), AuNP aggregates (B), AuNP aggregates digested by 8 U μL^{-1} Exo III (C), and AuNP aggregates incubated with 500 nM TATA binding protein followed by digestion by 8 U μL^{-1} Exo III (D).

internal standard for the Exo III-digested AuNP aggregates in the absence of TATA binding protein. This confirmed the degradation of the DNA-cross-linked AuNP aggregates by Exo III. After the AuNP aggregate incubated with TATA binding protein followed by extensive Exo III digestion, there was no noticeable peak appearing in the electropherograms for the supernatant. This observation is a little surprising, since it was anticipated that TATA binding protein could only protect the upstream sequence of its binding site, whereas the downstream four-nucleotide sequence might be degraded in Exo III-mediated digestion. As a matter of fact, the binding of TATA binding protein might substantially increase the steric hindrance in the DNA-cross-linked AuNP networks such that Exo III could not penetrate into the AuNP aggregates and digest the DNA strands in the networks. As a result, only very limited DNA sequences downstream of the binding sites at the surface of the DNA-cross-linked AuNP networks were degraded, and their concentrations were too low to be detected. When the observations in CE experiments were combined, we could infer that the dissociation of the DNA-cross-linked AuNP aggregates into dispersed AuNPs was arising from the degradation of DNA by Exo III, and the binding of DNA-binding proteins to its recognition sites could protect the AuNP aggregates from the degradation. This gave immediate evidence for the postulated mechanism of our Exo III protection-based colorimetric biosensor.

Additional evidence could be accomplished via dynamic light scattering (DLS) assay of the AuNP aggregates before and after Exo III-mediated digestion. As shown in Figure 7, the average hydrodynamic diameter of DNA-modified AuNPs was ~51.3 nm, and the average diameter of the AuNP aggregates was increased to ~615.1 nm. After Exo III-mediated degradation, the size of the AuNP aggregates decreased to ~73.8 nm, approaching the size of dispersed AuNPs. This implied that the AuNP aggregates were digested by Exo III into individually dispersed AuNPs or very small aggregates. However, the protection of the AuNP aggregates by TATA binding protein throughout Exo III-mediated degradation yielded an average diameter of ~521.3 nm, a size merely slightly smaller than that of the AuNP aggregates. This confirmed that

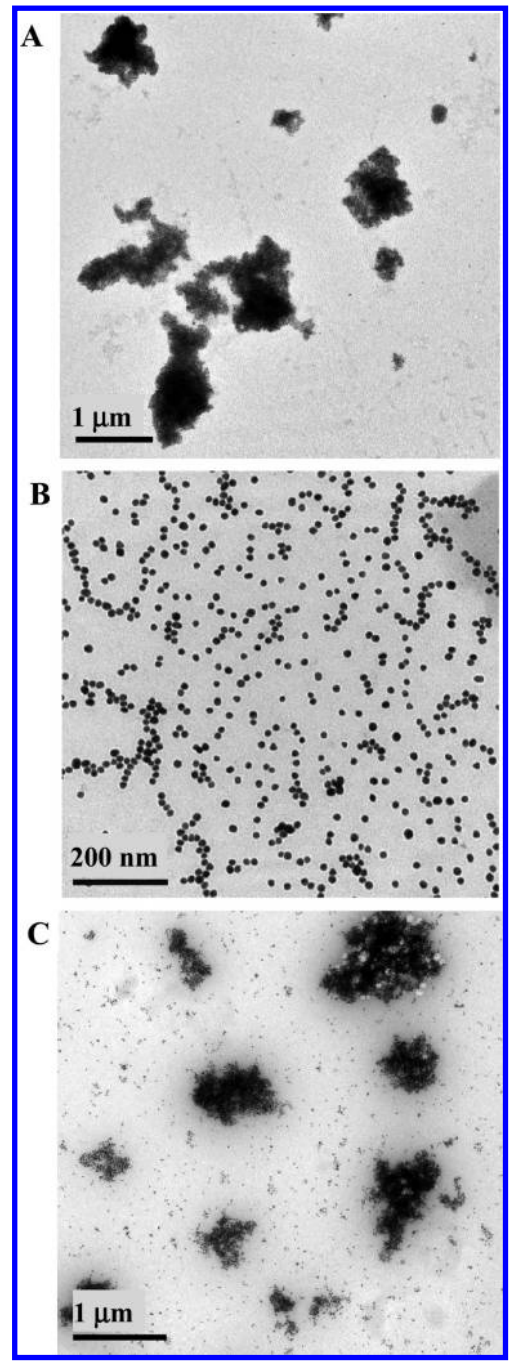

Figure 8. TEM images of DNA-cross-linked AuNP aggregates before the degradation (A) and after digestion by 8 U μL^{-1} Exo III in the absence (B) and presence (C) of 500 nM TATA binding protein.

the digestion of the AuNP aggregates by Exo III was prevented by the sequence-specific DNA−protein binding.

Transmission electron microscopy investigation was performed to further verify this finding. As shown in Figure 8, the TEM image of the AuNP aggregates after digestion by Exo III shows a majority of dispersed particles together with a minority of small aggregates. The size of these particles was 21 ± 8 nm. In contrast, in the presence of TATA binding protein, the digestion of the AuNP aggregates by Exo III also gave large aggregates of a few hundred nanometers in diameter. The size of AuNP aggregates was 465 ± 190 nm, which became slightly smaller than the size of AuNP aggregates as prepared via DNA cross-linking (530 ± 220 nm). This validated the protection of the DNA-cross-linked AuNP

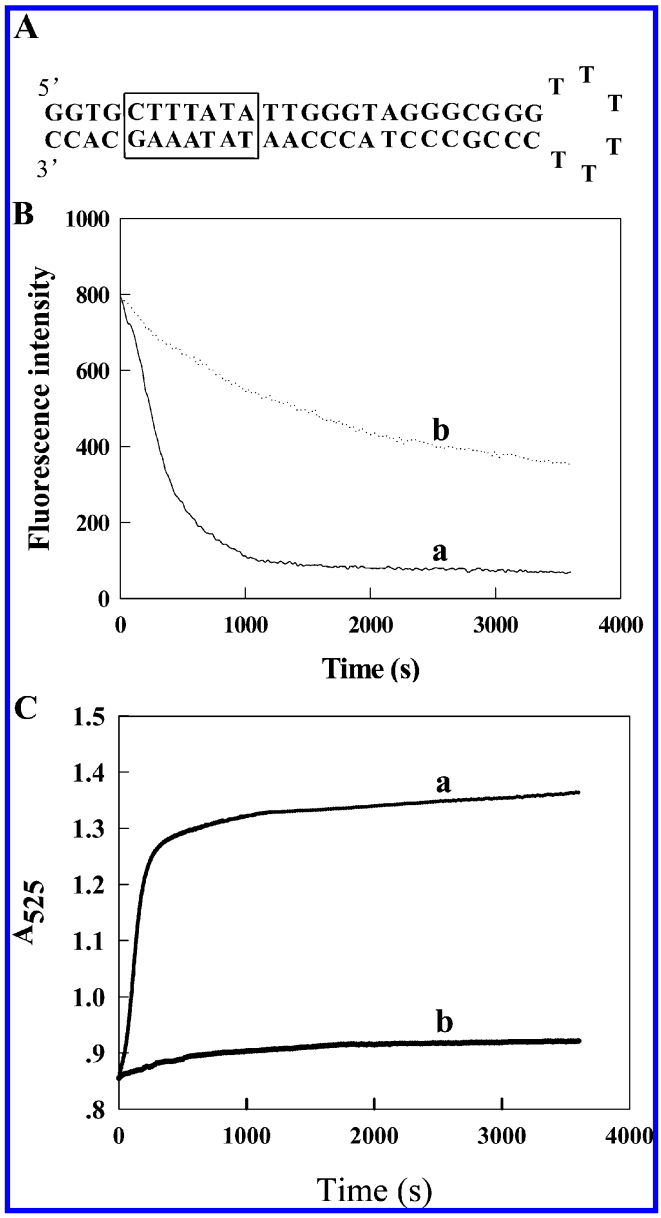

Figure 9. (A) Sequence of the hairpin-structured DNA. The black square indicates the protein-binding sites. (B) Time-dependent fluorescence emission intensity (λ_{ex} = 497 nm, λ_{em} = 525 nm) obtained for the digestion of hairpin DNA by Exo III in the absence (a) and presence (b) of 500 nM TATA binding protein. The concentrations of hairpin DNA and Exo III were 20 nM and 8 U mL^{-1}, respectively. (C) Time-dependent absorbance at 525 nm obtained for the digestion of AuNP aggregates by Exo III in the absence (a) and presence (b) of 500 nM TATA binding protein. The concentration of Exo III was 8 U μL^{-1}. The solution was agitated continuously throughout the detection.

aggregates from the Exo III digestion by interacting with TATA binding protein.

A most interesting finding obtained was that the protection of the DNA-cross-linked AuNP networks was sufficiently stable and lasted for a reasonably long period. This was contrasted substantially with the temporal protection of non-cross-linked double-stranded DNA in fluorescence assays.[14,15] To demonstrate clearly the distinction, we designed an Exo III protection-based homogeneous fluorescence assay for the detection of TATA binding protein (Figure 9). The assay utilized a hairpin-structured DNA with a stem sequence containing the consensus TATA binding protein-binding site (Figure 9A). SYBR Green I, a dye specifically intercalating DNA double-strands, was used to stain the stem and afford a fluorescence signal. After introducing 8 U mL^{-1} Exo III into the system with 20 nM hairpin DNA and excessive SYBR Green I (500-fold dilution), Exo III degraded the stem sequence from the 3′-terminal with SYBR Green I released. Then, it was observed that the fluorescence intensity decreased rapidly and became leveled off after 15 min (Figure 9B). Note that the concentration of Exo III was 1000-fold diluted in this fluorescence assay as compared to that used in our colorimetric biosensor. This low concentration was commonly used and essential for the detection of target proteins in Exo III protection-based fluorescence assays.[14,15] In the presence of 500 nM TATA binding protein, the fluorescence intensity decreased slowly and continuously over 1 h, indicating that the binding of the hairpin DNA by TATA binding protein merely inhibited the degradation rate by Exo III; no stable protection was achieved in such a system. In contrast to the fluorescence assay, the presence of 500 nM TATA binding protein gave a stable protection of the DNA-cross-linked AuNP aggregates, and the absorbance at 525 nm did not display appreciable time-dependent variations over 1 h under agitation conditions (Figure 9C). These results revealed that the colorimetric strategy offered more complete and stable inhibition of Exo III-mediated degradation than the fluorescence assay. Actually, this finding implied our assay could achieve a static color transition indicator for DNA−protein binding and require no time-dependent monitoring of the reaction. Hence, this strategy was expected to afford improved technical robustness and operational convenience as compared to the fluorescence assay. Actually, the stability of Au−DNA networks against nuclease digestion depended on the competition of protein binding with Exo III digestion. If protein displayed a much faster binding rate and slower dissociation rate than Exo III, then a "long-time" stabilization of Au−DNA networks was achieved. Presumably, such a stable protection might be attributed to the unique three-dimensional network structure formed by the DNA-cross-linked AuNP aggregates. This Au−DNA network presented very severe steric hindrance to Exo III digestion, while merely generating little steric hindrance to DNA-binding proteins. (The lateral orientation of DNA-binding proteins in recognizing the DNA duplex made the proteins farther away from the AuNP surface than Exo III that approached the 3′-end along the protruding strands.) As a result, in the Au−DNA networks Exo III digestion showed a much slower rate than protein binding, then a "long-time" stabilization of Au−DNA networks was observed. In other words, reversible binding of the protein to DNA was still maintained in the Au−DNA networks, and the "long-time" stabilization was attributed to the dominant kinetics of protein binding over that of Exo III digestion in the Au−DNA networks.

Quantitative Nature of the Exo III Protection-Based Colorimetric Biosensor for TATA Binding Protein Detection. The ability of the presented colorimetric biosensor for quantitative detection of the sequence-specific DNA-binding protein was also investigated. A series of different concentrations of TATA binding protein were incubated with the AuNP aggregates at 37 °C for 30 min, and then Exo III was added and digested for 20 min at room temperature. Figure 10A shows the photograph of the AuNP aggregates after the digestion. It was observed that, with increas-

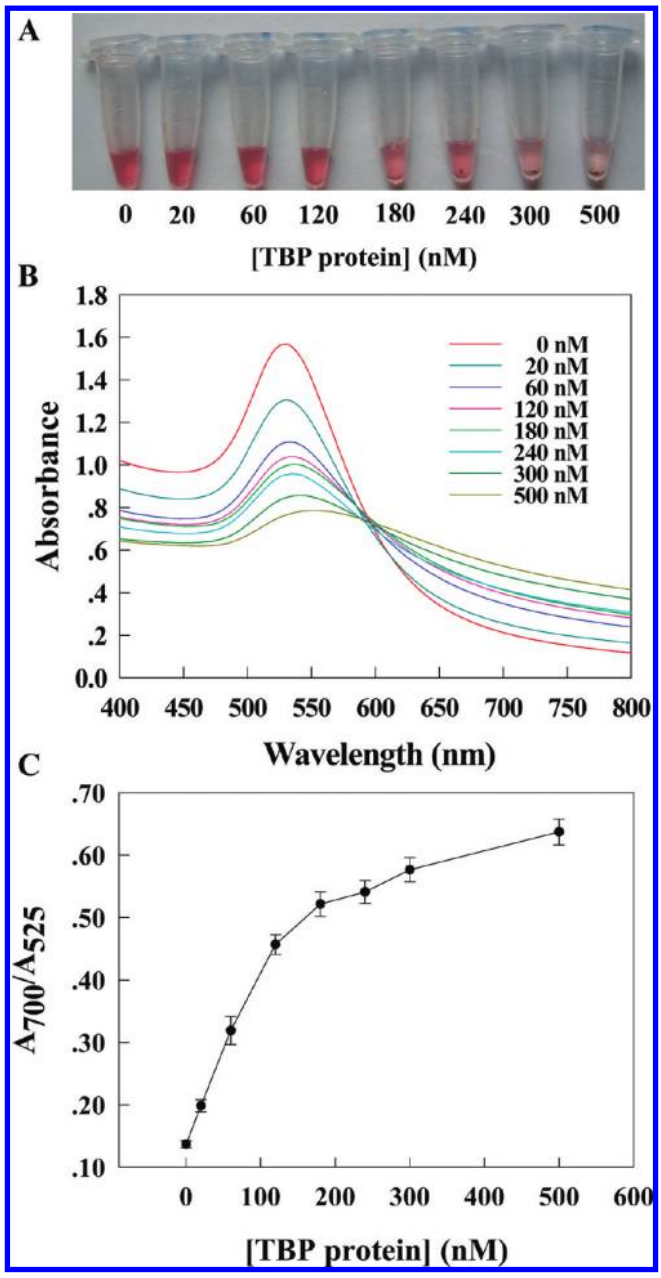

Figure 10. (A) Photograph of AuNP aggregates after incubation with different concentrations of TATA binding protein followed by digestion by 8 U μL^{-1} Exo III. (B) Absorption spectra of AuNP aggregates after incubation with different concentrations of TATA binding protein followed by digestion of 8 U μL^{-1} Exo III. (C) Plot of A_{700}/A_{525} vs TATA binding protein concentration. Error bars are SD across four repetitive experiments.

ing TATA binding protein concentration, the supernatants displayed colors with attenuated red, whereas the amount of purple-colored precipitates increased on the bottom of the microcentrifuge tubes. This suggested that more AuNP aggregates were protected from Exo III-mediated digestion in the presence of TATA binding protein of higher concentration. Figure 10B depicts the absorption spectra of the AuNP aggregates after Exo III-mediated digestion in the presence of different concentrations of TATA binding protein. It was clear that with increasing TATA binding protein concentration, the surface plasmon band gradually red-shifted and broadened, and the absorbance at 525 nm became decreased, whereas that at 700 nm increased, being quantitatively correlated to the concentrations of TATA binding protein. By plotting the ratios of the absorbances at 700 and 525 nm (A_{700}/A_{525}) versus TATA binding protein concentrations, a quasi-linear correlation was obtained in the concentration range from 0 to 120 nM (Figure 10C). The detection limit was estimated to be 10 nM, i.e., ~0.3 μg mL^{-1}, in terms of the rule of 3 times standard deviation over the blank response. This detection limit was better or comparable to those given by existing homogeneous assays based on fluorescence techniques,[12−15] which should be sufficient for detecting many DNA-binding proteins in cellular extracts.[13] Further improvement of the sensitivity could be achieved by optimizing the assay conditions such as the concentration of AuNP aggregates, the salt concentration, and the Exo III digestion time. Additionally, our method displayed favorable reproducibility. The relative standard deviation (RSD) for four repetitive assays using AuNP aggregates prepared in a single batch was ~4.3%, and the RSD for four assays using AuNP aggregates prepared in four different batches was ~5.4%. This revealed that the developed colorimetric biosensor held potentials for quantitative assay of the DNA-binding proteins with desirable sensitivity and reproducibility.

CONCLUSIONS

We developed a novel Exo III protection-based colorimetric biosensing strategy for rapid, sensitive, and visual detection of sequence-specific DNA-binding proteins. Our colorimetric biosensor provided several advantages over conventional approaches for DNA-binding protein assays. First, it allowed simple and direct visualization detection by using the "naked" eye, which circumvented the use of complicated instrumentation. Second, a static color transition indicator for DNA−protein interactions was achieved in the biosensing strategy with no time-dependent monitoring required. This furnished the developed strategy with improved technical robustness and operational convenience. It also solved the technical difficulty in conventional Exo III protection-based fluorescence assays, in which DNA could merely be temporally protected and time-dependent monitoring was frequently required. Third, a cyclic disulfide anchor of thioctic acid was introduced for tethering DNA strands on AuNPs. This improved the stability of the DNA-modified AuNPs and prevented the displacement of DNA by thiol compounds, thereby greatly expanding the potentials of AuNP-based colorimetric assays in enzyme systems. In addition, the developed approach can be further implemented for high-throughput assays using microplate formats. In view of these advantages, this new method holds great promise as a sensitive, specific, simple, and robust platform for quantitative assay of various sequence-specific DNA-binding proteins and the interactions between proteins and DNA.

ACKNOWLEDGMENT

This work was supported by the NSF (20975035) of China, the NSF of Hunan Province (07JJ3017), and the "973" National Key Basic Research Program (2007CB310500).

Received for review February 21, 2010. Accepted June 6, 2010.

AC100907G